

# CALPHAD and Phase-Field Modeling: A Successful Liaison

I. Steinbach, B. Böttger, J. Eiken, N. Warnken and S. G. Fries

(Submitted October 26, 2006)

The connection between CALPHAD models and Phase-Field models is discussed against the background of minimization of the total Gibbs energy of a system. Both methods are based on separation of a multiphase system into individual contributions of the bulk phases, which are described by appropriate models in composition, temperature, and pressure. While the CALPHAD method uses a global minimization of the total Gibbs energy, the Phase-Field method introduces local interactions, interfaces, and diffusion and allows for non-equilibrium situations. Thus, the Phase-Field method is much more general by its concept, however, it can profit a lot if realistic thermodynamic descriptions, as provided by the CALPHAD method, are incorporated. The present paper discusses details of a direct coupling between the Multiphase-Field method and the CALPHAD method. Examples are presented from solidification of technical Mg and Ni base alloys and some problems arising from common practice concerning thermodynamic descriptions in order-disorder systems.

**Keywords** CALPHAD, metastable phases, microstructure, phase transitions, Phase-Field modeling

## 1. Introduction

Thermodynamics deduces a maximum of information about a system with an infinite number of unknowns, only considering universal symmetries of nature. In this framework the time dependent Ginzburg-Landau theory forms the basis of modern Phase-Field models. However, it is rumored that even Landau himself did not believe his expansion of the free energy functional could be based on a serious physical background. As such we are in a neighborhood akin to CALPHAD modeling, whose “lack of physics” has often been blamed in the past, in particular by the honorary person of this symposium, Alan Oates.<sup>[1]</sup>

We welcome the recent efforts, to put “more physics into CALPHAD”, to combine CALPHAD with Ab initio

This article was presented at the Multi-Component Alloy Thermodynamics Symposium sponsored by the Alloy Phase Committee of the joint EMPMD/SMD of the Minerals, Metals, and Materials Society (TMS), held in San Antonio, Texas, USA, March 12-16, 2006, to honor the 2006 William Hume-Rothery Award recipient, Professor W. Alan Oates of the University of Salford, UK. The symposium was organized by Y. Austin Chang of the University of Wisconsin, Madison, WI, USA, Patrice Turchi of the Lawrence Livermore National Laboratory, Livermore, CA, USA, and Rainer Schmid-Fetzer of the Technische Universität Clausthal, Clausthal-Zellerfeld, Germany.

**I. Steinbach, B. Böttger, J. Eiken, and N. Warnken**, RWTH-Aachen, ACCESS e.V., Intzestr 5, 52072 Aachen, Germany; **S.G. Fries**, SGF Scientific Consultancy, Arndtstr. 9, 52064 Aachen, Germany and Equipe Physico-chimie des Matériaux Organisés Fonctionnels, Université Montpellier II, Institut C. Gerhardt, UMR-CNRS 5253, Montpellier, France. Contact e-mail: i.steinbach@access.rwth-aachen.de

methods<sup>[2]</sup> and to derive Phase-Field models by systematic coarse graining from density functional theory.<sup>[3-5]</sup> In the mean time, however, we try to demonstrate, how good physics can be made by the combination of both methods and how they can profit from each other.

Let us remember first, that the Ginzburg-Landau functional  $F = F(\phi, \nabla\phi)$  is an expansion in the order parameter  $\phi$  and its gradient  $\nabla\phi$  around a fixpoint, the critical point of a second order phase transformation. The justification of this expansion is, that both  $\phi$  and  $\nabla\phi$  vanish at the critical point and are small in its close vicinity. The expansion parameters, or Landau coefficients, are related to the distance from the critical point and reflect the universal symmetries of the system under consideration. The overwhelming success of this concept lasts on in the renormalization group theories of phase transitions. When applying the concept to first order phase transitions, the principle feature of the system, to be scale invariant, is lost. Finite size effects and the intrinsic properties of the system become important. Now the Landau parameters need to be related to measurable quantities. The break through in this respect marks the birth of the Phase-Field approach, when Caginalp<sup>[6]</sup> and later Wheeler et al.<sup>[7]</sup> worked out the Gibbs-Thomson limit of the Phase-Field equation, which relates the Landau parameters to interface mobility, energy, and width and to the free energy difference between bulk phases. Following their line we formulate the Ginzburg-Landau free energy functional  $F$  composed of the grain boundary part  $f^{\text{GB}}$  and the chemical part  $f^{\text{CH}}$  (other contributions like elastic and magnetic energy may be added)

$$F = \int_{\Omega} f^{\text{GB}} + f^{\text{CH}} \quad (\text{Eq 1})$$

$$f^{\text{GB}} = \sum_{\alpha, \beta=1}^N \frac{4\sigma_{\alpha\beta}}{\eta} \left\{ \frac{\eta^2}{\pi^2} |\nabla\phi_{\alpha} \cdot \nabla\phi_{\beta}| + \phi_{\alpha}\phi_{\beta} \right\} \quad (\text{Eq 2})$$

## Section I: Basic and Applied Research

$$f^{\text{CH}} = \sum_{\alpha=1}^N \phi_{\alpha} f_{\alpha}(\vec{c}_{\alpha}) + \bar{\mu} \left( \vec{c} - \sum_{\alpha=1}^N \phi_{\alpha} \vec{c}_{\alpha} \right) \quad (\text{Eq 3})$$

$\phi_{\alpha}(x; t)$  is the Phase-Field variable,  $\phi_{\alpha} = 1$  if the local state of the system is phase  $\alpha$ ,  $\phi_{\alpha} = 0$  if the phase is not  $\alpha$ . The intermediate values 0 mark the interface regions.  $\sigma_{\alpha\beta}$  is the grain boundary energy between a grain of phase  $\beta$  and  $\alpha$  grain of phase  $\beta$ ,  $\eta$  the interface width, here taken equal for all pairs of phases<sup>[1]</sup>  $f_{\alpha}(c_{\alpha}^i)$  is the bulk Gibbs free energy of phase  $\alpha$  with concentration  $\vec{c}_{\alpha}$  and  $\bar{\mu}$  is the diffusion potential  $\bar{\mu} = (\bar{f}_{\alpha}/c_{\alpha}) = (\bar{f}_{\beta}/c_{\beta})$  equal in all coincident phases. It was a long way from the general Ginzburg-Landau models to the thermodynamic consistent models in the Gibbs-Thomson limit, and there are still numerous theoretical, numerical, and practical aspects open. However, the identification of the model parameters to those given above, is well established today. Kim et al.<sup>[8]</sup> were the first to point out that the bulk free energy terms  $f_{\alpha}(\vec{c}_{\alpha})$  can be directly taken from CALPHAD databases, while the first numerical model, that used direct coupling to CALPHAD databases,<sup>[9]</sup> still used a phase diagram description with equilibrium slopes as a loop way. Now several models of coupling Phase-Field and CALPHAD have been published that differ in the treatment of the interface thermodynamics and in technical details of the coupling.<sup>[10-15]</sup> In the following we shortly summarize the actual model developed by the authors.<sup>[16]</sup> In Section 3 some demands on the databases will be discussed, that are crucial for their use in connection with Phase-Field calculations, before some example calculations are presented in Section 4.

## 2. Equations of Motion and Coupling Scheme

From the free energy model 1 we derive the Phase-Field and diffusion equation by relaxation in non-conserved and conserved formulation, respectively.<sup>[16-19]</sup>

$$\dot{\phi}_{\alpha} = \sum_{\beta} \mu_{\alpha\beta} [\sigma_{\alpha\beta}^* K_{\alpha\beta} + \Delta G_{\alpha\beta}] \quad (\text{Eq 4})$$

$$\dot{\vec{c}} = \nabla \sum_{\alpha=1}^N \phi_{\alpha} \mathbf{D}_{\alpha} \nabla \vec{c}_{\alpha}(\phi_{\beta}, \vec{c}) \quad (\text{Eq 5})$$

$$K_{\alpha\beta} = \phi_{\alpha} \nabla^2 \phi_{\beta} - \phi_{\beta} \nabla^2 \phi_{\alpha} + \frac{\pi^2}{\eta^2} (\phi_{\alpha} - \phi_{\beta}) \quad (\text{Eq 6})$$

$$\Delta G_{\alpha\beta} = -f_{\alpha}(\vec{c}_{\alpha}) + f_{\beta}(\vec{c}_{\beta}) + \bar{\mu}(\vec{c}_{\alpha} - \vec{c}_{\beta}) \quad (\text{Eq 7})$$

$\mu_{\alpha\beta}$ ,  $\sigma_{\alpha\beta}^*$  are the interface mobility and the interface stiffness.  $K_{\alpha\beta}$  is the generalized curvature term,  $\Delta G_{\alpha\beta}$  the thermodynamic driving force, and  $\mathbf{D}_{\alpha}$  the multi-component diffusion matrix for phase  $\alpha$ . The required phase concentrations  $\vec{c}_{\alpha}$  can be determined from the Phase-Field parameters and the total concentrations using the constraint of mass balance  $\vec{c} = \sum \phi_{\alpha} \vec{c}_{\alpha}$  and the equality of diffusion potential between coincident phases (two phases in a grain boundary, three in

a triple junction, and so on). Since during transformation the interfaces in the Phase-Field model are subject to a non-vanishing energy deviation from equilibrium  $\Delta G_{\alpha\beta}$ , we call this situation a quasi-equilibrium. To calculate the quasi-equilibrium phase concentrations  $c_{\alpha}$  in general, a thermodynamic minimization is required. However, doing this in every time-step for all interface cells is very time-consuming. To speed up simulations, thermodynamic calculations are only run after certain intervals and the quasi-equilibrium data is extrapolated in between. Starting from a set of quasi-equilibrium phase concentrations  $\vec{c}_{\alpha}^*$  and the respective temperature  $T^*$  for each pairwise phase interaction in each cell of the numerical grid, a new set of  $\vec{c}_{\alpha}$  is extrapolated. Using the abbreviations  $\Delta \vec{c}_{\alpha}$ ,  $\Delta \vec{c}_{\beta}$ , and  $\Delta T$  for the differences between extrapolated and starting values, the quasi-equilibrium constraint is considered by

$$\Delta \vec{c}_{\beta} = k_{\beta\alpha} (\Delta \vec{c}_{\alpha} \vec{q}_{\alpha\beta} \Delta T) + \vec{q}_{\beta\alpha} \Delta T \quad (\text{Eq 8})$$

with the quasi-equilibrium partition matrix  $k_{\beta\alpha}$ ,

$$k_{\beta\alpha}^{ij} = \left( \frac{\partial c_{\beta}^j}{\partial c_{\alpha}^i} \right)_{c_{\alpha}^{\neq i}, T}, \vec{q}_{\alpha\beta} = \left( \frac{\partial \vec{c}_{\alpha}}{\partial T} \right)_{c_{\beta}}, \vec{q}_{\beta\alpha} = \left( \frac{\partial \vec{c}_{\beta}}{\partial T} \right)_{c_{\alpha}}$$

All coefficients are evaluated and stored from thermodynamic quasi-equilibrium calculations, varying the concentrations  $c_{\alpha}^i$ , and the temperature independently.  $\vec{c}_{\alpha}$  can be extrapolated for changed Phase-Field parameters, changed total concentrations, and changed temperatures from the starting set of phase concentrations  $\vec{c}_{\alpha}^*$  by

$$\vec{c}_{\alpha}(\vec{c}\Phi_{\beta}T) = k_{\alpha c}^{-1} \vec{c} - \vec{c}_{\alpha}^{**}(\Phi_{\beta}T) \quad (\text{Eq 9})$$

with  $k_{\alpha c} = \sum_{\beta} \Phi_{\beta} k_{\beta\alpha}$  and

$$\vec{c}_{\alpha}^{**} = \sum_{\beta} \Phi_{\beta} (\vec{c}_{\beta}^* \vec{q}_{\alpha\beta} \Delta T - k_{\beta\alpha} (\vec{c}_{\alpha}^* + \vec{q}_{\beta\alpha} \Delta T))$$

## 3. Thermodynamic Database Aspects

The thermodynamic databases constructed using the CALPHAD method are sets of parametric functions describing the composition, temperature, and pressure dependence of the Gibbs energies for all the stable phases of a given system. The availability of these functions allows the calculation of multi-phase, multi-component equilibria at any temperature, composition, and pressure by the minimization of the total Gibbs energy for given conditions. In our Phase-Field calculation this minimization is used as a tool and applied to situations which differ from the ones used in equilibrium thermodynamics. First, and most important, the phase fractions of all phases coincident in one numerical cell is prescribed by the set of Phase-Field functions  $\{\phi_{\alpha}\}$ . Thus the system is over constrained and a solution can be found only with a finite offset  $\Delta G_{\alpha\beta}$  between

the phases (see Eq (7)). In strong non-equilibrium cases, typically during initialization of a new phase, this offset can be very large. Second, this leads to the fact that almost every database access is in an off equilibrium situation and reliable descriptions for the metastable phases and extensions of phase equilibria into metastable regions are needed. As experimental data here are hardly available,<sup>[20]</sup> good theoretical models are needed to extrapolate data into those regions. The databases should specially be checked to assure that the models give some reasonable behavior also in the metastable region.<sup>[21,22]</sup> The use of sound physical models should be more trustworthy in metastable extrapolations than mere numerical models. The use of additional parameters than the ones that can be determined by the experimental data in constructing the database usually leads to uncontrolled model artifacts in the unknown regions and therefore the number of parameters should be kept small and linked to some physical trends. Lastly, the third aspect is the treatment of phases for which the Gibbs energy has a miscibility gap, if it is defined by different compositions sets (ex: fcc-A1 in Ag-Al-Cu), or if it undergoes an order/disorder transformation (ex: L12  $\gamma'$ /A1  $\gamma$  in Al-Ni). If the system is far from equilibrium and the  $\Delta G_{\alpha\beta}$  offset is large it happens, that a description of the ordered phase is needed in the region where it is disordered. Extrapolation is then no longer possible, the only description available would be the disordered one.

Figure 1 shows the fcc phase diagram for Al-Ni which is modeled with a single Gibbs energy function taking into account the long-range ordering and describing the short-range ordering. Note that in the equilibrium phase diagram the function stable in the L1<sub>0</sub> range of composition is the bcc ordered phase, B2. Figure 2 shows the Gibbs energy for L1<sub>2</sub> and A1 in the binary Al-Ni system. Note, that the energy differences are very tiny and the separation of the

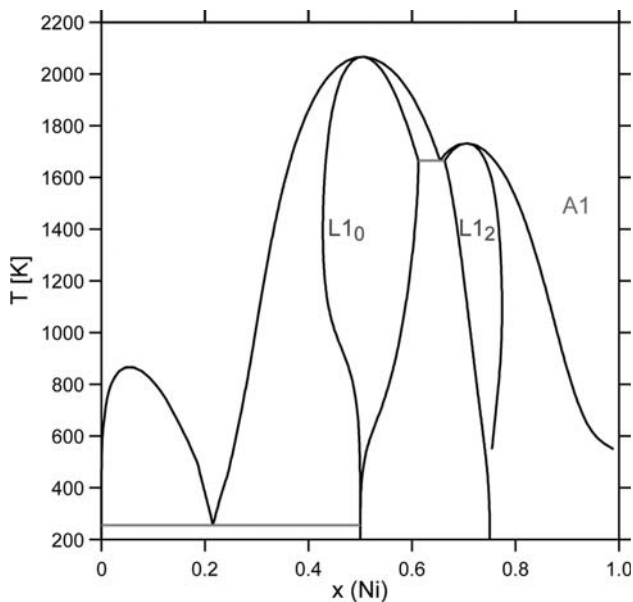


Fig. 1 Al-Ni FCC metastable phase diagram

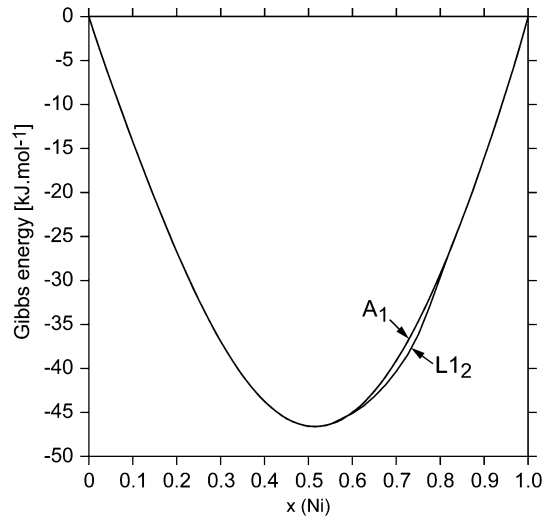


Fig. 2 L12 and A1 Gibbs energy at 1200 K

phases needs a high numerical accuracy. An alternative Phase-Field model, that uses the chemical ordering parameter as an independent Phase-Field variable is described in Ref 11. It seems, however, difficult to generalize this approach for general multi-phase problems.

## 4. Examples

### 4.1 Superalloy Solidification

The simulation of solidification microstructure formation in Ni-base superalloys poses a special challenge for thermodynamic-coupled Phase-Field simulation, not only because superalloys are multi-component alloys, but also due to the chemical order/disorder transformation of the alloys and the resulting CALPHAD modeling, as mentioned before. Single crystal superalloys are commonly Ni-base alloys, with Al as the main alloying element and smaller additions of Ta, Cr, Ti, W, Re, or other. The results presented here were calculated for a model superalloy, consisting of Ni-11.54 at.%Al-10.5 at.%Cr-2.6 at.%Ta-2.9 at.%W. Gibbs energies are taken from a database from Dupin, diffusion data from the NIST mobility database.<sup>[23]</sup> Interfacial energies are:  $\sigma_{\gamma\gamma'} = 10 \text{ mJ/m}^2$  and  $\sigma_{\gamma\text{liq}} = 30 \text{ mJ/m}^2$ . The interface mobilities are chosen to fulfill the diffusion-controlled limit. During solidification Al, Cr, and Ta segregate to the melt, while W enriches in the dendrite core. The solidification microstructure consists of primary  $\gamma$  dendrites and interdendritic  $\gamma'$  which forms through a peritectic reaction from the melt and the  $\gamma$ -dendrites. The formation of interdendritic  $\gamma'$  occurs only due to segregation. As has been recently shown, the interdendritic  $\gamma'$  nucleates from the primary  $\gamma$  dendrites at the solid-liquid interface.<sup>[24]</sup> Figure 3 shows results obtained from the simulation of solidification for a thermal gradient  $G = 20 \text{ K/mm}$  and a solidification velocity of  $v = 5 \text{ mm/min}$ . Shown is the W distribution over two dendrite trunks with interdendritic  $\gamma'$ . The W enrichment in the dendrite core

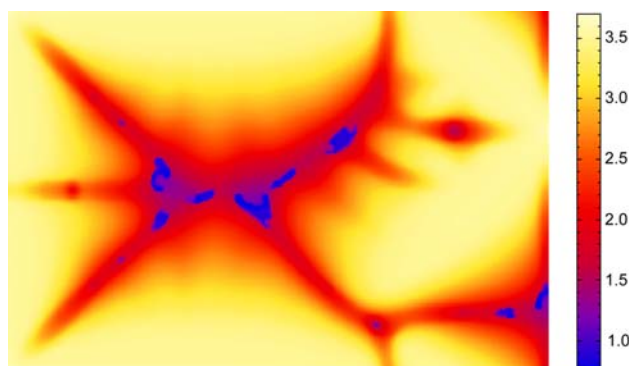


**Fig. 3** Simulated tungsten distribution in the region between two dendritic trunks. W is enriched in the solid during solidification (bright yellow means high W content) and depleted in the liquid (dark blue). There the  $\gamma'$  (blue spots) forms in a peritectic transformation at the end of the solidification. Calculation by MICRESS<sup>[25]</sup>

is directly visible. The interdendritic  $\gamma'$  dissolves almost no W and thus  $\gamma'$  is visible as blue spots.

During the calculation of this microstructure a number of pitfalls show up. Understanding these is necessary to find workarounds. When the primary solidification starts, just the  $\gamma$  phase is stable, equilibrium calculations predict the formation of  $\gamma'$  from  $\gamma$  well below the solidus temperature. In the thermodynamic database used for the simulation both phases are modeled with the same Gibbs energy function. When  $\gamma'$  starts to order, the Gibbs energy of the ordered phase is augmented by an ordering term. As a consequence metastable  $\gamma$  can be found over the whole composition range, while  $\gamma'$  appears as the ordered phase only under a very limited range of conditions (see Fig. 2). Outside this range  $\gamma'$  behaves exactly like  $\gamma$ . During the calculation the phases are named, e.g., fcc#1 and fcc#2, usually in the order of their order of stability. Thus the name of a phase is not permanently associated with the thermodynamic description and initializing the phase interaction at the very beginning of the simulation results in obtaining the same phase description for both phases. In our Phase-Field model it is necessary to associate one phase description uniquely to one Phase-Field parameter. That is obviously not possible under these circumstances. Once the initialization went wrong, it can only be recovered by restarting the simulation. The workaround applied here is to delay the initialization of the  $\gamma'$  until the composition in the melt and the temperature reaches the point, where ordered  $\gamma'$  forms are ordered. This is approximately the point for which also Scheil calculation predicts the formation of  $\gamma'$ . Once fine tuning the use of the database for the Phase-Field calculation very successful simulations are possible.

#### 4.2 Solidification of Mg alloy AZ31

A successful combination of thermodynamic database assessment and Phase-Field calculation can be reported for the magnesium alloy AZ31. The thermodynamic description of Mg-Al-Mn system has been improved by focusing on Mn-solubility in Mg-Al liquid, which is reported in Ref 26.

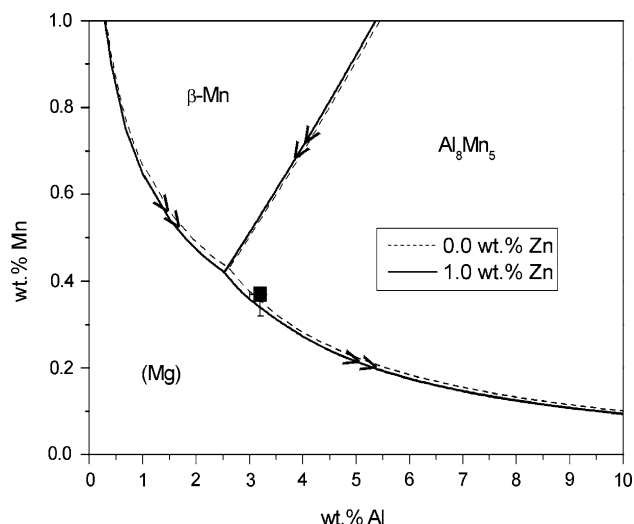


**Fig. 4** Calculated primary crystallization fields for Mg-Al-Mn alloys (dashed line) and quaternary Mg-Al-Mn-Zn with 1% Zn. The square mark indicates the composition of the AZ31 alloy. From Ref 27

It has been clarified that the solidification process in most of Mg-rich Mg-Al-Zn alloys proceeds close to the Scheil conditions. As for Mg-Mn-Zn system, it has been shown that there are some inconsistencies in the reported experimental works and the present thermodynamic calculation describes more reasonable phase equilibria, especially, the invariant reaction associated with the solidification of Mg-alloys. Shown in Fig. 4 are calculated projections of the liquidus surface, indicating primary crystallization fields (from Ref 27). These are separated by the monovariant three-phase reaction lines for liquid in equilibrium with two primary precipitates. The arrows indicate the direction of the reaction line along which the temperature decreases, and the primary precipitates are specified in the figure. The dashed lines correspond to the calculated result for Mg-Al-Mn ternary alloy, while the bold lines represent the result for Mg-Al-Mn-Zn with constant 1 wt.% Zn in the liquid alloy. It should be stressed that these are described with quite a high degree of accuracy based on the most reliable experimental data. One can see that the addition of 1 wt.% Zn has no significant effect on these monovariant reaction lines. More importantly, it can be realized that the AZ31 alloy is in a delicate composition range with three possible primary precipitates.

For the following simulation of constrained directional growth a temperature gradient  $G = 10$  K/mm in vertical direction and a growth velocity of 9 mm/min were chosen, the width of the calculation domain is 2 mm. To verify the reproduction of anisotropic behavior initial seeds with three different orientations were set ( $0^\circ$ ,  $15^\circ$ ,  $30^\circ$  disorientation to the temperature gradient). The given situation leads to complex dendritic structures, with the local growth orientations being physically predefined by the hexagonal anisotropy and the individual grain orientations. Figure 5 shows the resulting microstructure after 23 s of growth.



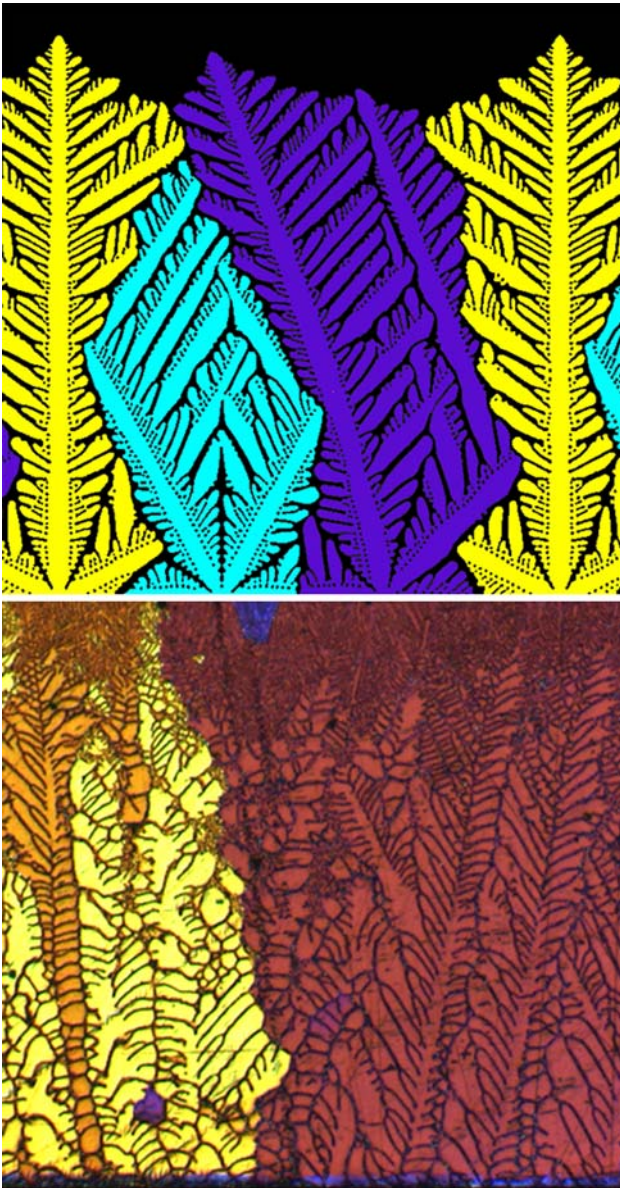


**Fig. 5** Simulations of directional growth of AZ31 in comparison with experiments<sup>[28]</sup> shall serve for calibration of inaccurate material data and as benchmark for anisotropic behavior. Calculation by MICRESS<sup>[25]</sup>

Significantly the angles between dendrite stem and arms are  $60^\circ$  because of the hexagonal structure of the crystal lattice of Magnesium. The evaluated growth orientations are in good agreement with the expected values, with a maximum deviation of  $2\text{--}3^\circ$ , which proves not only the functionality of the anisotropy formulation, but also the fact that unwanted numerical grid anisotropy has been reduced to a high degree,<sup>[27]</sup> though it can never be fully avoided in Phase-Field simulation. A rough comparison between simulations and experiments shows that the primary spacing differs by approximately a factor of two, which may be due to the fact that the evaluated simulations were far from a steady state or due to an incorrect surface energy and stiffness of the

solid-liquid interface, for which no reliable data are available. Nevertheless, the simulations show the right order of magnitude for the scale of the microstructure, dependent on the growth conditions as prescribed by temperature gradient and cooling rate and interdendritic segregation of solute which follows closely the partitioning as calculated from the database information.

## 5. Conclusions

A Phase-Field model coupled to CALPHAD databases is presented shortly. Its main feature is the use of a quasi-equilibrium construction for the partitioning of a solute at interphases and a  $\Delta G_{\alpha\beta}$  offset between the tangent lines on the Gibbs energy curves, that defines the kinetic driving force of the interphase motion. Some issues related to the use of standard CALPHAD data bases within this scheme are discussed, that are:

- Reliability of Gibbs energies in metastable regions and metastable extensions of equilibrium lines.
- Easy and consistent identification of the individual phases by their ordering status.
- Splitting the Gibbs energy of a phase with a miscibility gap into two hypothetical Gibbs energies. Applications in solidification of a Ni-base alloy with formation of interdendritic  $\gamma'$  and solidification of AZ31 Mg alloy, using a newly assessed database are demonstrated.

## Acknowledgments

We like to thank Dr. N. Dupin for providing information for the Ni database and the German research foundation (DFG) for financial support under the integrated project SPP1168 and the collaborative research center SFB370.

## References

1. W. A. Oates, H. Wenzel, and T. Mohri, Putting More Physics into Calphad Solution Models, *CalPhad-computer Coupling of Phase Diagrams and Thermochemistry*, 1996, **20**, p 37-45
2. B. P. Burton, N. Dupin, S. G. Fries, G. Grimvall, A. F. Guillermet, P. Miodownik, W. A. Oates, and V. Vinograd, Using ab initio calculations in the CALPHAD environment, *Z. Metallk.*, 2007, **92**, p 514-525
3. K. R. Elder and M. Grant, Modeling Elastic and Plastic Deformations in Nonequilibrium Processing using Phase-Field Crystals, *Phys. Rev. E*, 2004, **70**, p 051605-1-051605-18
4. N. Goldenfeld, B. P. Athreya, and J. A. Dantzig, Renormalization Group Approach to Multiscale Simulation of Polycrystalline Materials using the Phase-Field Crystal Model, *Phys. Rev. E*, 2005, **72**, p 020601-1-020601-4
5. M. G. A. Tjssens and G. D. James, Towards an Improved Continuum Theory for Phase Transformations, *Mat. Sci. Eng. A*, 2004, **378**, p 453-458
6. G. Caginalp and P. Fife, Phase-Field Methods for Interfacial Boundaries, *Phys. Rev. B*, 1986, **33**, p 7792-7794
7. A. A. Wheeler, W. J. Boettinger, and G. B. McFadden, Phase-Field Model for Isothermal Phase Transitions in Binary Alloys, *Phys. Rev. A*, 1992, **45**, p 7424-7439

## Section I: Basic and Applied Research

8. S. G. Kim, W. T. Kim, and T. Suzuki, Phase-field Model for Binary Alloys, *Phys. Rev. E*, 1999, **60**, p 7186-7197
9. U. Grafe, B. Böttger, J. Tiaden, and S. G. Fries, Coupling of Multicomponent Thermodynamic Databases to a Phase-Field Model: Application to Solidification and Solid State Transformations of Superalloys, *Scripta Mat.*, 2000, **42**, p 1179-1186
10. P.-R. Cha, D.-H. Yeon, and J.-K. Yoon, A Phase-Field Model for Isothermal Solidification of Multicomponent Alloys, *Acta Mat.*, 2001, **49**, p 3295-3307
11. J. Z. Zhu, Z. K. Liu, V. Vaithyanathan, and L. Q. Chen, Linking Phase-Field Model to CALPHAD: Application to Precipitate Shape Evolution in Ni-base Alloys, *Acta Mat.*, 2002, **46**, p 401-406
12. H. Kobayashi, M. Ode, S. G. Kim, W. T. Kim, and T. Suzuki, Phase-Field Model for Solidification of Ternary Alloys Coupled with Thermodynamic Database, *Scripta Mat.*, 2003, **48**, p 689-694
13. R. S. Qin and E. R. Wallach, A Phase-Field Model Coupled with a Thermodynamic Database, *Acta Mat.*, 2003, **51**, p 6199-6210
14. D. Y. Li, S. Choudhury, Z. K. Liu, and L.-Q. Chen, Effect of External Mechanical Constraints on the Phase Diagram of Epitaxial  $\text{PbZr}_{1-x}\text{Ti}_x\text{O}_3$  Thin Films – Thermodynamic Calculations and Phase-Field Simulations, *Appl. Phys. Lett.*, 2003, **83**, p 1608-1610
15. K. Wu, Y. A. Chang, and Y. Wang, Simulating Interdiffusion Microstructures in Ni-Al-Cr Diffusion Couples: A Phase-Field Approach Coupled with Calphad Database, *Scripta Mat.*, 2004, **50**, p 1145-1150
16. J. Eiken, B. Böttger, and I. Steinbach, Multi Phase-Field Approach for Alloy Solidification, *Rev. E*, 2006, **73**, p 066122-1-066122-9
17. I. Steinbach, F. Pezzolla, B. Nestler, M. Seeelberg, R. Prieler, G. J. Schmitz, and J. L. L. Rezende, A Phase-Field Concept for Multiphase Systems, *Physica D*, 1996, **94**, p 135-147
18. J. Tiaden, B. Nestler, H. J. Diepers, and I. Steinbach, The Multiphase-Field Model with an Integrated Concept for Modeling Solute Diffusion, *Physica D*, 1998, **115**, p 73-86
19. I. Steinbach and F. Pezzolla, A Generalized Field Method for Multiphase Transformations using Interface Fields, *Physica D*, 1999, **134**, p 385-393
20. J. H. Perepezko and G. Wilde, Alloy Metastability During Nucleation-Controlled Reactions, *Ber. Bunsenges. Phys. Chem.*, 1998, **102**, p 1074-1082
21. S. G. Fries and B. Sundman, Development of Multicomponent Thermodynamic Databases for Use in Process Modelling and Simulations, *J. Phys. Chem. Sol.*, 2005, **66**, p 226-230
22. R. Schmid-Fetzer, A. Janz, J. Gröbner, and M. Ohno, Aspects of Quality Assurance in a Thermodynamic Mg Alloy Database, *Adv. Eng. Mater.*, 2005, **7**, p 1142-1149
23. C. E. Campbell, W. J. Boettinger, and U. R. Kattner, Development of Diffusion Mobility Database for Ni-Base Super alloys, *Acta Mat.*, 2002, **50**, p 775-792
24. N. Warnken, D. Ma, M. Mathes, and I. Steinbach, Investigation of Eutectic Island Formation in SX Superalloys, *Mat. Sci. Eng. A*, 2005, **413-414**, p 267-271
25. <http://www.micress.de>
26. M. Ohno and R. Schmid-Fetzer, Thermodynamic Assessment of Mg-Al-Mn Phase Equilibria, Focusing on Mg-rich Alloys, *Z. Metallk.*, 2005, **96**, p 857-869
27. B. Böttger, J. Eiken, M. Ohno, G. Klaus, M. Fehlbier, R. Schmid-Fetzer, I. Steinbach, and A. Bührig-Polazcek, Controlling Microstructure in Magnesium Alloys: A Combined Thermodynamic, Experimental and Simulation Approach, *Adv. Eng. Mat.*, 2006, **8**(4), p 241-247
28. G. Klaus and A. Bührig-Polazcek, Unpublished research at Foundry Institute Aachen, 2005